

EQUILIBRIUM AND KINETICS STUDIES FOR THE ADSORPTION OF CRYSTAL VIOLET DYE BY *SPIRULINA PLATENSIS*

UZMA NADEEM, ARUN KANT & PANMEI GAIJON

Department of Chemistry, University of Delhi, Delhi, India

ABSTRACT

Equilibrium and kinetics of the sorption of the Crystal Violet dye on *Spirulina platensis* was studied. The pH stability of the dye was also studied. The equilibrium sorption data were fitted into Langmuir, Freundlich and Temkin isotherms. Freundlich adsorption isotherm fitted well as the R^2 value of Freundlich isotherm model was the highest. The maximum monolayer coverage (q_{max}) from Langmuir isotherm model was determined to be 126.28 mg g^{-1} . For the Freundlich isotherm model, the sorption intensity (n) is 1.33, which indicates favourable sorption. The heat of sorption process was calculated from Temkin Isotherm model is 50.27 J mol^{-1} , which proved that the adsorption experiment followed a physical process. Adsorption kinetic data were applied on the best fitted model was pseudo second order kinetics with highest R^2 and K_2 values for pseudo-second-order are 0.99 and 15.8479 mg/g respectively, indicating maximum equilibrium adsorption capacity for pseudo-second-order kinetics. The intra-particle diffusion model was also applied.

KEYWORDS: Biosorption, Crystal Violet Dye, Isotherm, Kinetics, *Spirulina platensis*

INTRODUCTION

The generation of hazardous dye, organic chemical, heavy metal and toxic material containing effluents discharge in the water body leads to the formation of contaminated wastewater. Worldwide, nearly 1 million tonnes of synthetic dyes are produced annually [1, 2]. The textile industry is responsible for the use of 30% of synthetic dyes [3]. In recent years, more than 100,000 dyes are available in market. It is necessary to remove dyes from their effluents before discharging [4]. The dye-containing wastewater from these industries cause adversely effect on aquatic environment by impeding light penetration and inhibiting the photosynthesis of aqueous flora [5] and aquatic biota [6]. The effects of these dyes can result in allergy, dermatitis, skin irritation [7] and also induce cancer [8], mutation in humans [9] and harmful to human health [10]. Many methods have been employed to remove synthetic dyes from industrial effluents [11,12]. One of the unitary operation most often used for the removal of synthetic dyes from industrial effluents is the adsorption procedure [13], due to its simplicity and high efficiency, as well as the availability of a wide range of adsorbents. Conventional methods are expensive, ineffective for color removal, and less adaptable to a wide range of dye wastewaters [14]. Biosorption is an alternative eco-friendly technology for removal of color from aqueous solutions, due to ease of operation, complete removal of pollutants, even from dilute solutions [15]. Biosorption has more capacity for uptake of pollutants from aqueous solutions by the use of non-growing or dead microbial biomass. Now a days different kinds of biosorbents have been used to remove dyes from aqueous solutions have been reported in the literature, like fungi, bacteria, *Azolla rongpong* [16], *Aspergillus parasiticus* [17], and *Nostoc linckia* [18], cupuassu shell [5], jujuba seeds [19], chitosan [20], algae [21]. *Spirulina platensis* is a member of blue-green algae, contains a variety of functional groups such as carboxyl, hydroxyl,

sulfate, amine, phosphate and other charged groups on the surface which can be mediate pollutant binding [22]. It is available in large quantities and cultivated worldwide; its annual production is about 2000 tons [23, 24]. This alga was also successfully employed for removal of chromium, cadmium and lead from aqueous solutions [25, 26]. Crystal violet dye extensively used in animal and veterinary medicine as a biological stain and in various commercial textile operations [27]. It is carcinogenic and poorly metabolized by microbes, is non-biodegradable, and can persist in a variety of environments [28].

This present study deals with the adsorption equilibrium and kinetic studies for the adsorption of Crystal Violet Dye from an aqueous solution using *Spirulina platensis*.

MATERIALS AND METHODS

Materials

Organic dye crystal violet is a cationic dye. C.I. number 42555, molecular weight 407.99 and molecular formula $C_{25}H_{30}ClN_3$ was procured from Thomas Baker Chemical Limited Mumbai. All the chemicals used throughout this study were of analytical-grade reagents and the adsorption experiments were carried out at room temperature (30 °C).

Methods

Stock solutions were prepared with the known concentration of dye. The pH of the aqueous solution was adjusted using the solutions 0.1N, 1N HCl and 0.1N, 1N NaOH solution. In the pH stability study, CV dye stability was observed at pH 5. In the adsorption experiments, the dye solution was centrifuged and the maximum dye absorbance in the filtrate was measured at the maximum wave length (586 nm) via UV-Vis spectrophotometer. In the pH effect study maximum adsorption of dye was observed at pH 6 and due to this all the experiments were performed at pH 6 but the absorbance was recorded at pH 5 because of the stability of dye at pH 5. The molecular structure and absorbance peak of CV at 586 nm are shown in Figure 1A and 1B respectively.

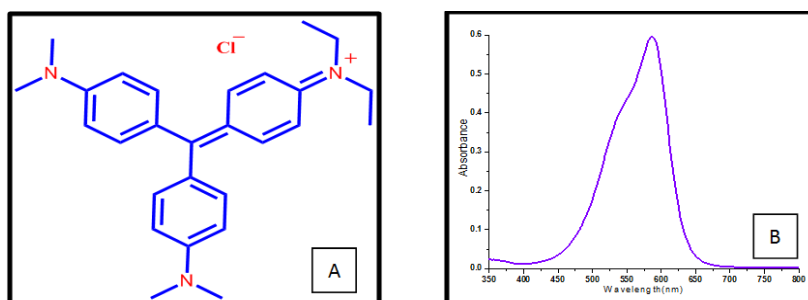


Figure 1: Crystal Violet Dye (A) Molecular Structure and (B) Absorption Spectra

For the equilibrium isotherm studies initial dye concentration taken between 10-100 mg L^{-1} with 25 mg adsorbent dose and the pH 6 was adjusted for the aqueous solution. In terms of kinetic studies the variables that were used during the experiments are contact time (5, 10, 15, 20, 25, 30, 40, 50, 60 and 80 minute), the amount of adsorbent is 25 mg for dye concentration 20 mg L^{-1} at pH 6.

Data Analysis

The basic approaches were used in interpreting the experimental result for adsorptive capacity. The percent Adsorption efficiency of CV was determined for each sample of *Spirulina platensis* at the same equilibrium points as follows [29, 30]. The amount of CV dye free in the solution was determined from corresponding Beer-Lambert plot.

The percentage efficiency of the CV dye on adsorbent was calculated was using the equation 1:

$$R\% = \frac{(C_i - C_e)}{C_i} 100 \quad (1)$$

The amount of crystal violet adsorbed onto adsorbent, q_e (mg g^{-1}), was calculated using the equation 2:

$$q_e = \frac{(C_i - C_e)V}{W} \quad (2)$$

Where, q_e is the CV dye uptake (mg g^{-1}), C_i is the initial concentrations (mg L^{-1}), C_e is equilibrium concentrations of CV dye (mg L^{-1}), V the volume of CV dye solution (L) and W the weight of adsorbent (g).

The residual dye concentration was determined and the amount of CV dye adsorbed, at time t was calculated using the equation:

$$q_t = \frac{(C_i - C_e)V}{W} \quad (3)$$

Where, q_t is the CV dye uptake at time t (mg g^{-1}).

RESULTS AND DISCUSSIONS

Adsorption Isotherms

Adsorption isotherms are mathematical models that describe the distribution of the adsorbate species among liquid and adsorbent, based on a set of assumptions that are mainly related to the heterogeneity/homogeneity of adsorbents, the type of coverage and possibility of interaction between the adsorbate species. Adsorption data are usually described by adsorption isotherms, such as Langmuir and Freundlich isotherms. These isotherms relate dye uptake per unit mass of adsorbent, q_e , to the equilibrium adsorbate concentration in the bulk aqueous phase C_e .

Freundlich Adsorption Isotherm

Freundlich isotherm is describing the non-ideal and reversible adsorption, not restricted to the formation of monolayer. At present, Freundlich isotherm [31] is widely applied in heterogeneous systems especially for organic dye and compounds or highly interactive species on natural material or adsorbent. The slope $1/n$ ranges between 0 and 1 is a measure of adsorption intensity or surface heterogeneity for normal adsorption, becoming more heterogeneous as its value gets closer to zero. Whereas, a value below unity implies chemisorptions process, If $n = 1$ then the partition between the two phases are independent of the concentration. $1/n$ above one is an indicative of cooperative adsorption [32,33]. Freundlich isotherm is commonly used to describe the adsorption characteristics of the heterogeneous surface [34]. The non-linearized Freundlich can be written as equation 3:

$$q_e = K_f C_e^{1/n} \quad (3)$$

Where K_f = Freundlich isotherm constant (mg g^{-1}), n = adsorption intensity, C_e = the equilibrium concentration of adsorbate (mg L^{-1}) and q_e = the amount of dye adsorbed per gram of the adsorbent at equilibrium (mg g^{-1}).

Linearized equation of Freundlich isotherm:

$$\log q_e = \log K_f + \frac{1}{n} \log C_e \quad (4)$$

The plot of $\log q_e$ versus $\log C_e$ is linear (Figure 2) with a slope equal to $1/n$ and an intercept equal to $\log K_f$. The constant K_f is an approximate indicator of adsorption capacity, while $1/n$ is a function of the strength of adsorption.

Langmuir Adsorption Isotherm

This describes quantitatively the formation of a monolayer adsorbate on the outer surface of the adsorbent, and after that no further adsorption takes place [35, 36]. Thereby, the Langmuir represents the equilibrium distribution of crystal violet dye ions between the solid and liquid phases [37]. In its formulation, this empirical model assumes monolayer adsorption (the adsorbed layer is one molecule in thickness), with adsorption can only occur at fixed number of definite localized sites, that are identical and equivalent, with no lateral interaction between the adsorbed molecules, even on adjacent sites [38]. Moreover, Langmuir theory has related rapid decrease of the intermolecular attractive forces to the rise of distance. The Langmuir isotherm is valid for monolayer adsorption onto a surface containing a finite number of identical sites. The model assumes uniform energies of adsorption onto the surface and no transmigration of the adsorbate in the plane of the surface. Based upon these assumptions, the Langmuir isotherm equation may be expressed in a linearized form as shown in equation (5):

$$\frac{C_e}{q_e} = \frac{1}{q_{\max} K_L} + \frac{C_e}{q_{\max}} \quad (5)$$

Where, q_{\max} is the monolayer capacity of the adsorbent (mg/g) and K_L is the Langmuir adsorption constant (dm^3/mg).

The plot of C_e/q_e versus C_e is linear (Figure 3) with a slope equal to $1/q_{\max}$ and an intercept equal to $1/(q_{\max} K_L)$.

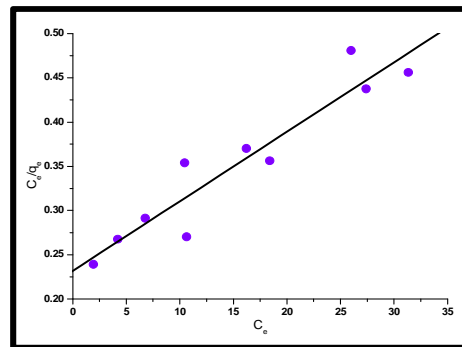


Figure 2: Linearized Plot for Freundlich Isotherms

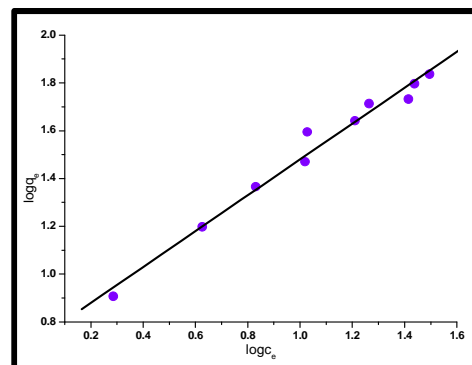


Figure 3: Linearized Plot for Langmuir Isotherm

The essential characteristics of the Langmuir equation can be expressed a dimensionless constant, commonly known as separation factor (R_L) defined by Webber [39] which given as:

$$R_L = \frac{1}{1 + K_L C_i} \tag{6}$$

Where, K_L ($L\ mg^{-1}$) refers to the Langmuir constant, C_i is indicated to the adsorbate initial concentration ($mg\ L^{-1}$). The magnitude of K_L also quantifies the relative affinity between an adsorbent and the adsorbent surface. In this context, lower R_L value reflects that adsorption is more favourable. In a most probable explanation, R_L value indicates the adsorption nature if $R_L > 1$ it indicate unfavourable, $R_L = 1$ it indicate linear, if $0 < R_L < 1$ it indicate favourable and if $R_L = 0$ it indicate irreversible adsorption. Figure 4 shows the separation factor $R_L < 1$ indicating a favourable.

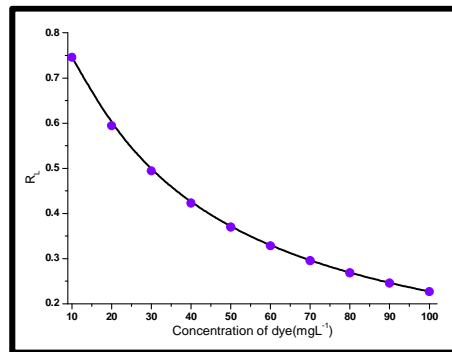


Figure 4: R_L vs Initial Dye Concentration

Temkin Adsorption Isotherm

Temkin isotherm is also describing the adsorption adsorption potentials of the CV onto *Spirulina platensis* in the aqueous solution. The Temkin isotherm [40] contains a factor that explicitly taking into the account of adsorbent–adsorbate interactions. By ignoring the extremely low and large value of concentrations, the model assumes that heat of adsorption of all molecules in a layer should decrease linearly rather than logarithmic with coverage [41]. A linear form of the Temkin isotherm equation can be expressed as:

$$q_e = B \log A + B \log C_e \tag{7}$$

Where R is gas constant (8.314 J/mol/K), T is Temperature (K) and $B = RT/b$. Adsorption data can be analyzed according to equation. (6). A plot of q_e versus $\log C_e$ plot of the Temkin isotherm is shown in Figure 5, gives the Temkin constants A and B.

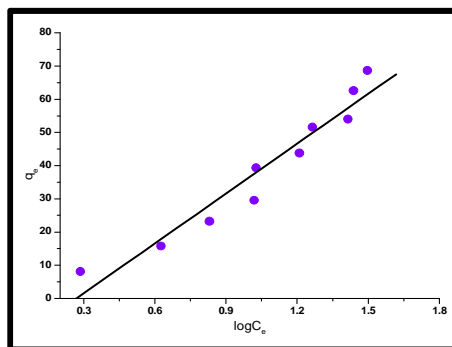


Figure 5: Linearized Plot for Temkin Isotherm

The constant parameters for Freundlich, Langmuir and Temkin isotherms are given in Table 1. Freundlich adsorption isotherm fitted well as the R^2 value of Freundlich isotherm model was the highest. From the data in table 1, that a value of $1/n$ and n indicating that the adsorption of crystal violet dye onto the *Spirulina platensis* is favourable. The maximum monolayer coverage (q_{max}) from Langmuir isotherm model was determined to be 126.28 mg g^{-1} , the separation factor indicating a favourable sorption experiment is 0.75. For the Freundlich Isotherm model, the sorption intensity (n) is 1.33, which indicates favourable sorption. The heat of sorption process was estimated from Temkin Isotherm model is 50.27 J mol^{-1} , which proved that the adsorption experiments followed a physical process.

Table 1: Freundlich, Langmuir and Temkin Isotherm Constants

Freundlich Parameters			Langmuir Parameters			Temkin Parameters		
$1/n$	K_f	R^2	$q_{max} (\text{mg g}^{-1})$	$K_L (\text{dm}^3 \text{mg}^{-1})$	R^2	$At (\text{dm}^3/\text{mg})$	$Bt (\text{J mol}^{-1})$	R^2
0.75	5.3691	0.9795	126.5823	0.0341	0.8953	2.7187	50.2702	0.9343

Adsorption Kinetics

Several steps can be used to examine the controlling mechanism of adsorption process such as chemical reaction and kinetic models are used to test experimental data from the adsorption of Crystal Violet onto *Spirulina platensis*. Several kinetic models are available to understand the behaviour of the adsorbent and also to examine the controlling mechanism of the adsorption process and to test the experimental data. In the present investigation, the adsorption data were analysed using three kinetic models, the pseudo-first-order, pseudo-second-order kinetic and the intra-particle diffusion models.

Pseudo-First-Order Equation

The pseudo-first-order model was presented by Lagergren [42, 43] which is the earliest known equation describing the adsorption rate based on the adsorption capacity. The differential equation is generally expresses a follows:

The Lagergren's first-order reaction model is expressed in linear form as equation (8):

$$\log(q_e - q_t) = \log q_e - \frac{K_1}{2.303} t \quad (8)$$

Where q_t and q_e are the amount adsorbed (mg g^{-1}) at time, t , and at equilibrium respectively and k_1 is the rate constant of the pseudo-first-order adsorption process (min^{-1}). Straight line plots of $\log(q_e - q_t)$ against t were used to determine the rate constant, K_1 , and correlation coefficients, R^2 , for different crystal violet dye concentrations with a slope of $-K_1/2.303$ and an intercept of $\log q_e$, as shown in Figure 6.

Pseudo-Second-Order Equation

The adsorption data was also analysed in terms of pseudo second order mechanism, described by Ho and McKay [44] can be used to explain the sorption kinetic. This model based on assumption. The linear form of the pseudo second order model shown in equation (9) as follows:

$$\frac{t}{q_t} = \frac{1}{K_2 q_e^2} + \frac{1}{q_e} t \quad (9)$$

Where K_2 is the rate constant of pseudo-second-order adsorption ($\text{mgg}^{-1} \text{min}^{-1}$), $K_2q_e^2$ is the initial rate of adsorption ($\text{mgg}^{-1} \text{min}^{-1}$). The second-order kinetics shows the plot t/q_t against t of equation (9), a linear relationship show in Figure 7. Values of K_2 and equilibrium adsorption capacity q_e were calculated from the intercept ($K_2q_e^2$) and slope ($1/q_e$) of the plots.

The Intra-Particle Diffusion Model

The intra-particle diffusion is another kinetic model should be used to study the rate of dye adsorption onto SP. The possibility of intra-particle diffusion was explored by using the intra-particle diffusion model. The adsorbate species are most probably transported from the bulk of the solution into the solid phase through intra-particle diffusion process, which is often the rate-limiting step in many adsorption processes, especially in a rapidly stirred batch reactor. Intra-particle diffusion model described by Weber and Morris [45] can be expressed by the following equation 10:

$$q_t = K_d t^{1/2} + C \tag{10}$$

The plot of q_t against $t^{1/2}$ gives a linear relationship with a slope of K_d and an intercept of $C(\text{mg g}^{-1})$ as shown in Figure 8. Where q_t is the amount of dye adsorbed (mg g^{-1}) at time t , K_d ($\text{mg g}^{-1} \text{min}^{1/2}$) is the rate constant for intraparticle diffusion.

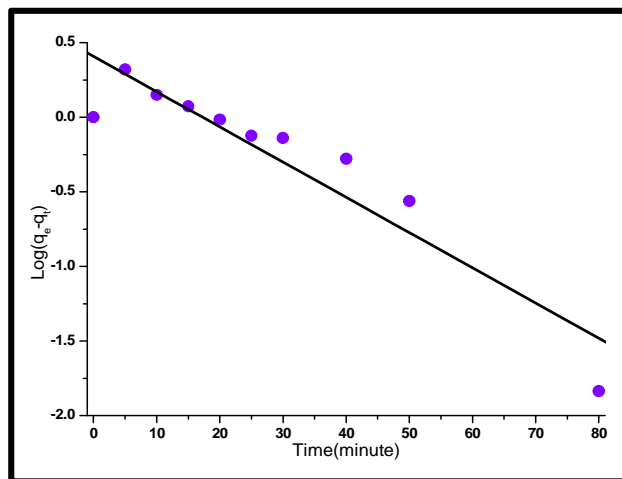


Figure 6: Pseudo-First-Order Kinetic Plot

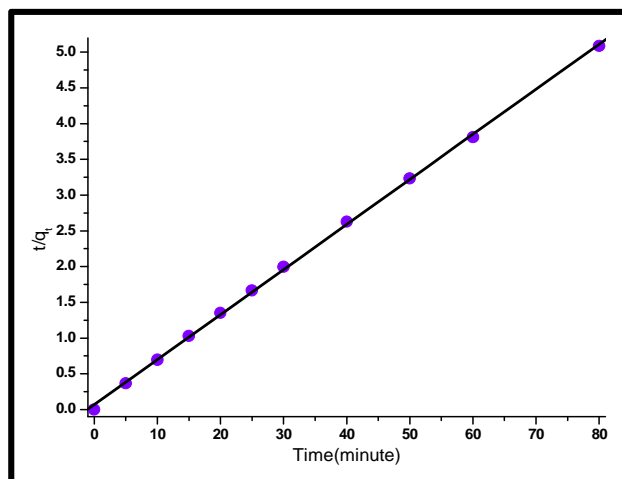


Figure 7: Pseudo-Second-Order Kinetic Plot

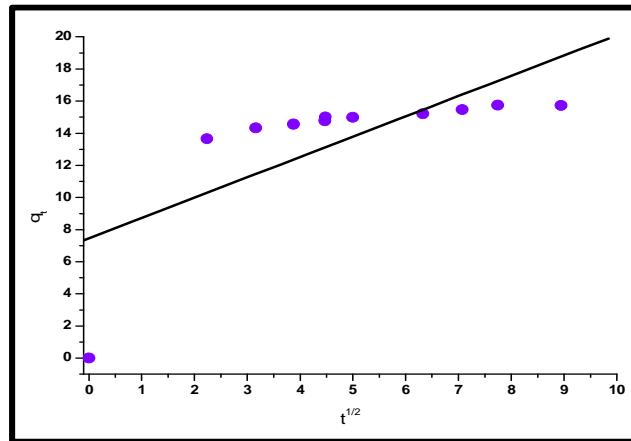


Figure 8: Intra-Particle Diffusion Plot

In the intra-particle diffusion model the constant C was increased with increasing the dye concentration, which indicating the increase of the thickness of the boundary layer and decrease of the chance of the external mass transfer and hence increase of the chance of internal mass transfer. The R^2 values given in table are close to unity indicating the application of this model. This may confirm that the rate-limiting step is the intra-particle diffusion process. The linearity of the plots demonstrated that intra-particle diffusion played a significant role in the uptake of the adsorbate by adsorbent.

Table 2: Pseudo-First-Order, Pseudo-Second-Order and Intra-Particle Diffusion Constants

Pseudo-First-Order			Pseudo-Second-Order			Intra-Particle Diffusion		
K_1 (min^{-1})	q_e (mg g^{-1})	R^2	K_2 [$\text{g}/(\text{mg min})$]	q_e (mg g^{-1})	R^2	K_d	C	R^2
0.0433	2.2558	0.6414	0.0579	15.8479	0.9995	1.2639	7.4637	0.515

Table 2 shows the calculated adsorption constants/parameter for pseudo-first-order, pseudo-second-order kinetic and the intra-particle diffusion models. It is clear from the table that the best fitted model was pseudo second order kinetics with highest R^2 value. K_1 and K_2 values for pseudo-first-order and pseudo-second-order are 0.0433 and 15.8479 mg/g respectively indicating maximum equilibrium adsorption capacity for pseudo-second-order kinetics and the best fitted model was pseudo second order kinetics with highest R^2 value. K_1 and K_2 values for pseudo-first-order and pseudo-second-order are 0.0433 and 15.8479 mg/g respectively indicating maximum equilibrium adsorption capacity for pseudo-second-order kinetics. In the intra-particle diffusion model the value of C is 7.46 mg g^{-1} indicating the increase of the thickness of the boundary layer and decrease of the chance of the external mass transfer and hence increase of the chance of internal mass transfer. This confirms that the rate-limiting step is the intra-particle diffusion process.

CONCLUSIONS

The study suggests that *Spirulina platensis* is an excellent adsorbent for the remediation of Crystal Violet dye from aqueous solutions. The experimental data in the adsorption studies were fitted well to Freundlich and Langmuir equations to determine the extent and degree of favourability of adsorption. Monolayer adsorption capacity is found to be 126.28 mg g^{-1} at 303K. The heat of sorption process was calculated from Temkin Isotherm model is 50.27 J mol^{-1} , which proved that the adsorption experiment followed a physical process. Adsorption kinetic data were applied on the best fitted model was pseudo second order kinetics with highest R^2 and K_2 values 0.99 and 15.8479 mg/g respectively indicating maximum equilibrium adsorption capacity for pseudo-second-order kinetics. Both intra-particle diffusion and surface adsorption contribute to the control of the rate of adsorption

ACKNOWLEDGEMENTS

Authors are thankful to the Head, Department of Chemistry, University of Delhi for departmental facilities and UGC [F.15-76/12 (SA-II)] for providing financial assistance.

REFERENCES

1. Singh K, Arora S. Removal of synthetic textile dyes from wastewaters: a critical review on present treatment technologies. *Crit. Rev. Env Sci. Technol* 2011; 4: 807–878.
2. Koprivanac N, Kusic H. *Hazardous Organic Pollutants in Colored Wastewaters*. New Science Publishers, 2009.
3. Hessel C, Allegre M, Maisseu F, Charbit PM. Guidelines and legislation for dye house effluents. *J Environ. Manage* 2007; 83, 171–180, 2007.
4. Mahmoodi, NM, Hayati, B., Arami, M. Textile dye removal from single and ternary systems using date stones: Kinetic, isotherm, and thermodynamic studies. *Journal of Chemical and Engineering Data* 2010; 55:4638-4649.
5. Cardoso NF, Lima EC, Pinto IS, Amavisca CV, Royer B, Pinto RB, Alencar WS, Perira SFP. Application of cupuassu shell as biosorbent for the removal of textile dyes from aqueous solution. *J Environ. Manage* 2011; 92:1237–1247.
6. Wan NWS, Teong LC, Hanafiah M. Adsorption of dyes and heavy metal ions by chitosan composites: a review. *CarbohydrPolym* 2011; 83:1446–56.
7. Brookstein DS. Factors associated with textile pattern dermatitis caused by contact allergy to dyes, finishes, foams, and preservatives. *Dermatol Clin.* 2009; 27:309–322.
8. Carneiro PA, Umbuzeiro GA, Oliveira DP, Zanoni MVB. Assessment of water contamination caused by a mutagenic textile effluent/dyehouse effluent bearing disperse dyes. 2010; *J Hazard. Mater* 174:694–699.
9. Lima ROA, Bazo AP, Salvadori DMF, Rech CM, Oliveira DP, Umbuzeiro GA. Mutagenic and carcinogenic potential of a textile azo dye processing plant effluent that impacts a drinking water source. *Mutat Res Genet. Toxicol. Environ. Mutagen* 2007; 626:53–60.
10. Yang Y, Wang G, Wang B, Li Z, Jia X, Zhou Q, Zhao Y. Biosorption of Acid Black 172 and Congo Red from aqueous solution by nonviable *Penicillium YW 01*: kinetic study, equilibrium isotherm and artificial neural network modeling. *Bioresour Technol.* 2011; 102:828–834.
11. Gupta VK, Suhas. Application of low-cost adsorbents for dye removal: a review. *J Environ. Manag* 2009; 90:2313–2342.
12. Mondal S. Methods of dye removal from dye house effluent: an overview, *Environ Eng. Sci* 2008; 25:383–396.
13. Royer B, Cardoso NF, Lima EC, Ruiz VSO, Macedo TR, Airoidi C. Organofunctionalized kenyaite for dye removal from aqueous solution. *J Colloid Interface Sci* 2009; 336:398–405.
14. Srinivasan A, Viraraghavan T. Decolorization of dye wastewaters by biosorbents: A review. *Journal of Environmental Management* 2010; 91:1915-1929.

15. Aksu Z, Tezer S. Biosorption of reactive dyes on the green alga *Chlorella vulgaris*. *Process Biochemistry* 2005; 40:1347-1361.
16. Padmesh TVN, Vijayaraghavan K, Sekaran G, Velan M. Application of *Azollarongpongon* biosorption of acid red 88, acid green 3, acid orange 7 and acid blue 15 from synthetic solutions. *Chemical Engineering Journal* 2006; 122:55-63.
17. Akar ST, Akar T, Çabuk A. Decolorization of a textile dye, reactive red 198 by *Aspergillus parasiticus* fungal biosorbent. *Brazilian Journal of Chemical Engineering* 2009; 26: 399-405.
18. Mona S, Kaushik A, Kaushik CP. Biosorption of reactive dye by waste biomass of *Nostoc linckia*. *Ecological Engineering* 2011; 37:1589-1594.
19. Somasekhara RMC, Sivaramakrishna L, Varada RA. The use of an agricultural waste material, Jujuba seeds for the removal of anionic dye (Congo red) from aqueous medium, *J Hazard. Mater* 2012; 203:118-127.
20. Piccin JS, Dotto GL, Vieira MLG, Pinto LAA. Kinetics, Mechanism of the Food Dye FD&C Red 40 Adsorption onto Chitosan. *J Chem. Eng Data* 2011; 56:3759-3765.
21. Kousha M, E. Daneshvar E, Sohrabi MS, Jokar M, Bhatnagar A. Adsorption of acid orange II dye by raw and chemically modified brown macroalga *Stoechospermum marginatum*. *Chem Eng. J* 2012; 192: 67-76.
22. Seker A, Shahwan T, Eroglu A, S. Yilmaz, Z. Demirel, M. Dalay, Equilibrium thermodynamic and kinetic studies for the biosorption of aqueous lead(II), cadmium(II) and nickel(II) ions on *Spirulina platensis*. *J Hazard. Mater* 2008; 154:973-980.
23. Elekli MAC, Yavuzatmaca M. Predictive modeling of biomass production by *Spirulina platensis* as function of nitrate and NaCl concentrations. *Bioresour Technol* 2009; 100:1847-1851.
24. Elekli AC, Yavuzatmaca M, Bozkurt H. An eco-friendly process: predictive modeling of copper adsorption from aqueous solution on *Spirulina platensis*. *J Hazard. Mater* 2010; 73: 123-129.
25. Chojnacka K, Chojnacki A, Gorecka H. Biosorption of Cr^{3+} , Cd^{2+} and Cu^{2+} ions by blue-green algae *Spirulina* sp: Kinetics, equilibrium and the mechanism of the process. *Chemosphere* 2005; 59: 75-84.
26. Seker A, Shahwan T, Eroglu A, Yilmaz S, Demirel Z, Dalay M. Equilibrium, thermodynamic and kinetic studies for the biosorption of aqueous lead(II), cadmium(II) and nickel(II) ions on *Spirulina platensis*. *Journal of Hazardous Materials* 2008; 154: 973-980.
27. Senthilkumaar S, Kalaamani P, Subburaam CV. Liquid phase adsorption of crystal violet onto activated carbons derived from male flowers of coconut tree. *J Hazard. Mater* 2006; 136:800-808.
28. Chen CC, Liao HJ, Cheng CY, Yen CY, Chung YC. Biodegradation of crystal violet by *Pseudomonas putida*. *Biotechnol. Lett* 2007; 29:391-396.
29. Nameni M, Mghadam MR, Arami M. Adsorption of hexavalent chromium from aqueous solutions by wheat bran. *International J of Environmental Science and Technology* 2008; 5(2):161-168.

30. Ogbonnaya O. Preparation and comparative characterisation of activated carbon from Nigeria subbituminous coal, palm kernel shell and cow bone. *J Chem. Soc. of Nigeria* 1992; 17(11):11-14.
31. Freundlich HMF. Over the adsorption in solution. *J Phys. Chem* 1906; 57:385–471.
32. Haghseresht F, Lu G. Adsorption characteristics of phenolic compounds onto coal-reject derived adsorbents. *Energy Fuels* 1998; 12:1100–1107.
33. Mohan S, Karthikeyan J. Removal of lignin and tannin color from aqueous solution by adsorption on to activated carbon solution by adsorption on to activated charcoal. *Environ Pollut* 1997; 97:183-187
34. Hutson ND, Yang RT. Adsorption. *J Colloid Interf Sci* 2000; 189.
35. Allen SJ, Mckay G, Porter JF. Adsorption isotherm models for basic dye adsorption by peat in single and binary component systems. *J Colloid Interface Sci* 2004; 280:322–333.
36. Demirbas E, Kobya M, Konukman AES. Error analysis of equilibrium studies for the almond shell activated carbon adsorption of Cr(VI) from aqueous solutions. *J Hazard. Mater* 2008; 154:787–794.
37. Vermeulan TH, Vermeulan KR, Hall LC. Fundamental. *Ind Eng. Chem* 1966; 5:212–223.
38. Vijayaraghavan K, Padmesh TVN, Palanivelu K, Velan M. Biosorption of nickel(II) ions onto *Sargassum wightii*: application of two-parameter and three parameter isotherm models. *J Hazard. Mater* 2006; 133:304– 308.
39. Webber TW, Chakkravorti RK. Pore and solid diffusion models for fixedbedadsorbents. *AIChE J* 1974; 20:228–238.
40. Tempkin MI, Pyzhev V. Kinetics of ammonia synthesis on promoted ironcatalyst. *Acta Phys. Chim* 1940; 12:327–356.
41. Aharoni C, Ungarish M. Kinetics of activated chemisorption. Part 2. Theoretical models. *J Chem. Soc. Faraday Trans* 1977; 73:456–464.
42. Lagergren S. About the theory of so called adsorption of soluble substances. *Handlingar Band* 1898;24: 1-39.
43. Chandra TC, Magdalena MM, Sunarso J, Sudaryanto Y, IsmadjiS. Activated carbon from durian shell: Preparation and characterization. *Journal of the Taiwan Institute of Chemical Engineers* 2009; 40(4):457-462.
44. Dotto GL, Lima EC, Pinto LAA. Biosorption of food dyes onto *Spirulina platensis* nanoparticles: equilibrium isotherm and thermodynamic analysis. *BioresourTechnol* 2012; 103:123–130.
45. Weber J, W J., Morris, JC. Kinetics of adsorption on carbon from solution, *Eng. Div. Proceed. Am. Soc. Civil. Eng* 1963;89:31–60

